The research on the size determination of electromagnetic suction force according to the air gap eccentricity in a vibration motor

UnChol Ri [A*], YongChol Ri [A], ChangIl Ri[A], CholJU Kim[B], GyongBong Ju[A], DaeSong O[A]

[A] Faculty of renewable Energy Science, Hamhung University of Hydraulics and Power, Hamhung, D P R of Korea
[B] KIM IL SUNG University, Pyongyang, D P R of Korea

[*] Correspondence: UnChol Ri, Hamhung University of Hydraulics and Power, Ham Hung, D P R of Korea
[+] E-mail address: riunchol@163.com

ARTICLE INFO

Keywords:
Air gap
Motor
Eccentricity

Abstract

In the paper, the dimension of the air gap eccentricity and the effect of the harmonic field considered. Also, based on this problem, the electromagnetic suction force acting on the rotor was accurately determined. Thus, it is possible to increase the structural reliability of the motor shaft and rotor at the design calculation stage.

1. Main contents

At present, three-phase asynchronous motors are the most frequently used electric equipment in various sectors of the economy. It is a very significant problem to improve production quality while reducing the manufacturing cost while increasing the quality index. In particular, the vibration motor used for sorting of coal in coal mines and mines is an electric machine that requires vibration during the operation process, and the eccentricity of the rotor appears severely during the operation process by the action of a vibration balance weight. Therefore, accurately determining the electromagnetic suction force according to the size of eccentricity has been raised as a very urgent problem.

So far, a simplified formula has used in the design of the vibration motor. Precisely, when the air gap eccentricity exists, the average value of the eccentric force acting on the shaft is determined and multiplied by the stability coefficient to determine the axis diameter. This method has a disadvantage with low reliability because of inconsideration with exactly electromagnetic attraction force of various components acting during operation.

In the paper, the dimension of the air gap eccentricity and the effect of the harmonic field considered. Also, based on this, the electromagnetic suction force acting on the rotor was accurately determined. Thus, it is possible to increase the structural reliability of the motor shaft and rotor at the design calculation stage. The electromagnetic eccentricity generated by the air gap eccentricity and the harmonic magnetic field in the vibration motor used for the coal sorter acts on the rotating body, causing the shaft to bend. The electromagnetic suction force acting on the rotor can be obtained as follows, according to Maxwell's definition.

$$p_r(\theta,t)=\frac{b^2(\theta,t)}{2\mu_0} \tag{1}$$

Where, μ_0 -Air relative magnetic permeability

$b(\theta,t)$ - Air gap Magnetic flux Density function

From Equation 1, it can see that the electromagnetic suction force acting on the rotor is proportional to the square of the magnetic flux density. The change function of the Air gap Magnetic flux Density $b(\theta,t)$ can be expressed as follows according to time t and angle θ.

$$b(\theta,t)=\frac{1}{\delta(\theta,t)} \tag{2}$$

Where, $\delta(\theta,t)$ - Variation function of Air gap size with time t and angle θ

When the rotor is eccentric, the relative eccentricity of the rotor can express as follows.

$$\varepsilon=\frac{e}{\delta} \tag{3}$$

Where, e - Rotor eccentricity, mm

δ -When $\varepsilon=0$, the space size is uniformly uniform, mm

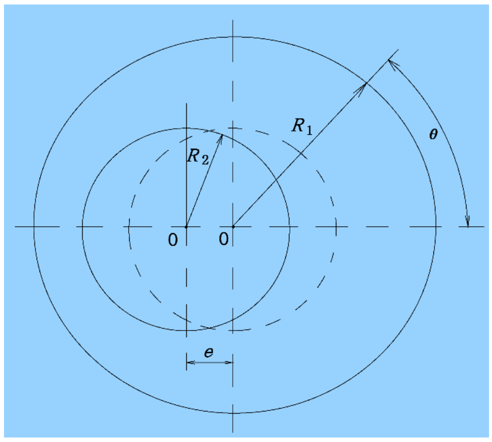

Figure 1. Structure of eccentric rotor

When the eccentric rotor rotates, the air gap changes with time t and the central angle θ .

Therefore, $\delta(\theta,t)$ can write as

$$\delta(\theta,t)=(R_1-R_2)-e\cos(\theta-\omega_2 t)=\delta\left[1-\varepsilon\cos(\theta-\omega_2 t)\right]=\delta k_e \tag{4}$$

Where, $\delta=R_1-R_2$, mm

R_1 - Stator inner diameter, mm

R_2 - Rotor outer diameter, mm

θ - The central angle of the force calculation point in the rotation circumference, °

ω_2 - Rotation angle frequency of rotor

In Equation 4, $k_e=\left[1-\varepsilon\cos(\theta-\omega_2 t)\right]$ is a side number reflecting the eccentricity and is a function according to θ, t, ε .

The air gap magnetization function in a regularly operated three-phase asynchronous motor is as follows.

$$f(\theta,t)=f_0(\theta,t)+\sum_{\nu} f_\nu(\theta,t)+\sum_{\mu} f_\mu(\theta,t)=F_0\cos(p\theta-\omega_1 t-\varphi_0)+ \\ +\sum_{\nu} F_\nu(\nu\theta-\omega_\nu t-\varphi_1)+\sum_{\mu} F_\mu(\mu\theta-\omega_\mu t-\varphi_2) \quad (5)$$

Where,

ν, μ - Stator, rotor harmonic order

ω_1 - Stator's fundamental wave rotation angular velocity, rad/s

ω_μ - Rotor μ-order harmonic wave angular velocity, rad/s

ω_ν - Stator ν-order harmonic wave angular velocity, rad/s

F_0 - The amplitude of the fundamental wave composite magnetization force, A

F_ν - The amplitude of the magnetization force of ν-order harmonic wave in the stator winding, A

F_μ -The amplitude of the magnetization force of μ-order harmonic wave in the rotor winding, A

In the case of eccentricity, air gap magnetic conductivity expressed as the following function.

$$\lambda(\theta,t)=\frac{\mu_0}{\delta(\theta,t)} \quad (6)$$

When the stator and rotor have grooves, the result of deriving the relationship of the change in magnetic flux density in the air gap considering the haircut magnetic conductivity is as follows.

$$b(\theta,t)\approx\begin{bmatrix} F_0\Lambda_0\cos(p\theta-\omega_1 t-\varphi_0)+\sum_{\nu z} F_{\nu z}\Lambda_0(\nu_z\theta-\omega_\nu t-\varphi_1)+ \\ +\sum_{\mu z} F_{\mu z}\Lambda_0\cos(\mu_z\theta-\omega_\mu t-\varphi_2)+\sum_{\nu z}\frac{F_0\Lambda_{k1}}{2}(\nu_z-\omega_\nu t-\varphi_{0\nu})+\sum_{\mu z}\frac{F_0\Lambda_{k2}}{2}(\mu_z-\omega_\mu t-\varphi_{0\mu}) \end{bmatrix} \quad (7)$$

Where,

Λ_0 - Constant component of magnetic conductivity, 1/s

$\Lambda_{k1}, \Lambda_{k2}$ - Magnetic conductivity considering stator and rotor haircuts, 1/s

p - Pole pairs

$F_{\nu z}$ - Stator tooth ν-order harmonic wave amplitude, A

$F_{\mu z}$ - Rotor tooth μ-order harmonic wave amplitude, A

From equations 1 to 7, the equation for calculating the radial electromagnetic attraction force considering the air gap eccentricity and harmonic wave field can express as follows.

$$p_n(\theta,\mathrm{t}) = \frac{b^2}{2\mu_0} = \frac{1}{2\mu_0}\begin{Bmatrix} \frac{B_1^2}{2}\cos(2p\theta - 2\omega_1\mathrm{t} - 2\omega_{0\nu}) + \sum_{\nu z}\sum_{\mu z} B_{\nu z}B_{\mu z}\cos[(\mu\pm\nu)\theta - \\ -(\omega_\mu \pm \omega_\nu)\mathrm{t} - (\omega_{\mu z} \pm \omega_{\nu z})] \end{Bmatrix} \quad (8)$$

Where,

$B_{\nu z}$ - The amplitude of stator tooth ν-order harmonic wave density, T

$B_{\mu z}$ -The amplitude of rotor tooth μ-order harmonic wave density, T

B_1 - The amplitude of fundamental wave synthesis magnetic flux density, T

From Equation 8, it is possible to determine the radial force acting on the rotor in an asynchronous motor with grooves and haircuts in the stator and rotor.

2. Experiment results and analysis using MATLAB

Using MATLAB, the pore magnetic flux density along the circumference of the rotor surface, the corresponding fundamental wave element force size, and the harmonic wave element force size was determined.

Fig. 2 shows the magnetic flux density distribution and electromagnetic suction force distribution according to the central angle θ in the rotational resource circumference calculated by Equation 8 when the eccentricity is given as 10% of the pore size.

In Figure 2, the x-axis is the central angle of the point where the radius direction electromagnetic attraction force calculated on the rotational circumference.

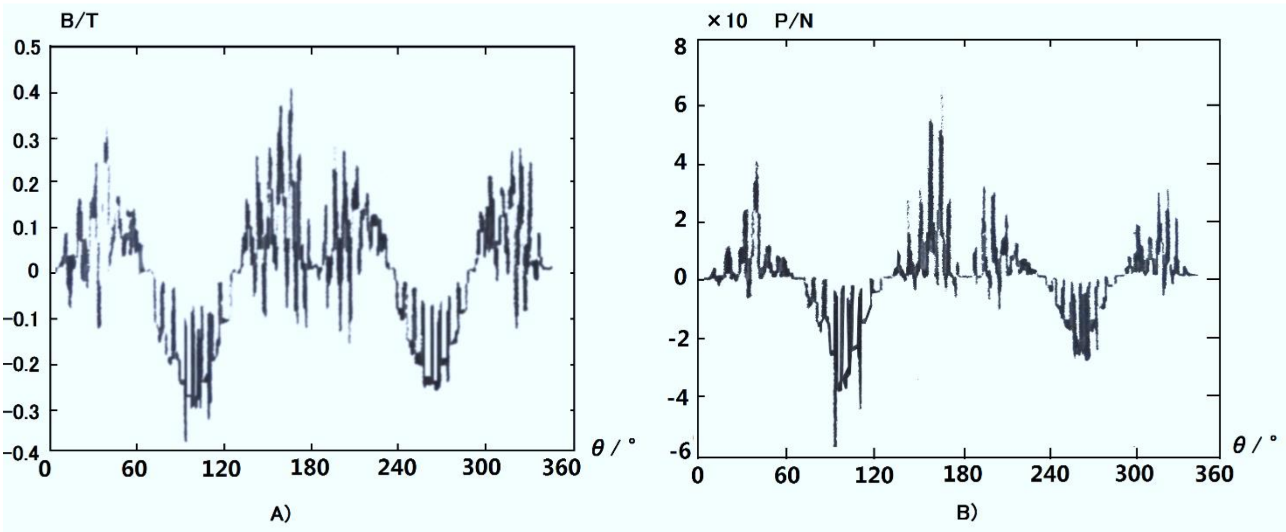

Fig2. The distribution of magnetic flux density and electromagnetic attraction according to the central angle in the rotational resource circumference

As shown in A) of Fig. 2, it can see that the distribution of pore magnetic flux density along the central angle θ includes many harmonics. And the pore magnetic flux density varies irregularly due to the eccentricity of the pores. That is, in the section from 90 ° to 270 °, the air gap is smaller than the standard air gap due to eccentricity, and the void magnetic flux density increased, and in the remaining section. So, the air gap increased, and the void magnetic flux density decreased.

In B of Fig. 2, the quantity of the electromagnetic suction power is distributed unevenly according to the distribution of magnetic flux density, and the resulting magnitude of the force increases in the section where the air gap reduced so that the electromagnetic suction force acts in one direction.

Table 1 shows the magnitudes of the harmonic wave component force, the fundamental wave component force, and the composite component force according to the size of the air gap eccentricity.

Table 1. The electromagnetic force acting on the rotor according to the air gap eccentricity

e, %	Harmonic component force, N	Basic wave component force, N	Synthetic, N	100* Harmonic component force / Synthetic, %
1	1.94	36.80	38.70	5.01
5	9.72	184.25	193.98	5.01
10	19.57	369.39	388.96	5.03
15	29.64	556.30	585.95	5.05

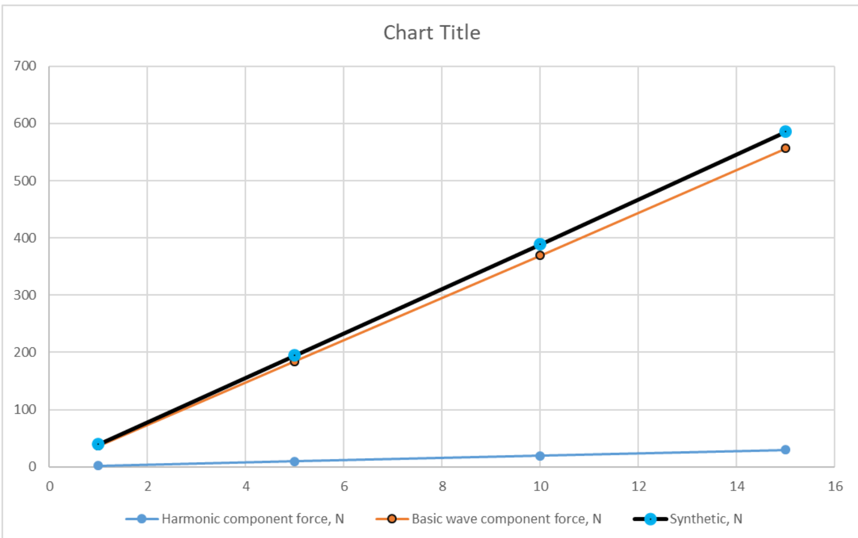

Fig3. The electromagnetic force acting on the rotor according to the air gap eccentricity

As shown in Table 1 and Fig3, it can see that the harmonic component force among electromagnetic attraction forces is within 5% of the composite component force. The synthetic component force of the electromagnetic suction force is combined with the eccentric power by the vibration weight to create bending stress on the rotor shaft.

Thus, in this paper, the design was conducted by accurately determining the electromagnetic suction force when the air gap eccentricity was maximized, thereby making it possible to manufacture a vibration motor for coal sorter that can guarantee the structural reliability of the shaft.

Acknowledgements

The authors wish to thank Mr. RI who gave us much valuable helping in the early stages of this work.

AUTHOR CONTRIBUTIONS

Authors equally contributed.

ORCID

UnChol Ri http://orcid.org/0000-0002-4474-3389

References

[1] Kanaan H Y, Al-Haddad K, Roy G. Analysis of the electromechanical vibrations in induction motor drives due to the imperfections of the mechanical transmission system [J]. Mathematics and Computers in Simulation, 2003, 63(3-5):421-433.

[2] Jang, G.H, Lieu, D.K. The effect of magnet geometry on electric motor vibration [J]. IEEE Transactions on Magnetics, 27(6):5202-5204.

[3] Ralph O. Eis. Electric Motor Vibration-Cause, Prevention, and Cure [J]. IEEE Transactions on Industry Applications, 1975, IA-11(3):267-275.

[4] Wang Jian, Zhang Lijun, Yu Zhuoping amp. An Analysis on the Vibration Order Feature of the Electric Motor Assembly in a Fuel Cell Car [J]. Automotive Engineering, 2009, 31(3):219-223.

[5] Sun, Wei, Li, Yinong, Huang, Jingying, et al. Vibration effect and control of In-Wheel Switched Reluctance Motor for electric vehicle [J]. Journal of Sound & Vibration, 338:105-120.

[6] Peicheng Shi, Yuan Shang. The Vibration Analysis of Eco-Friendly Vehicle Based on the Electric Motor Excitation[C]// 2012.

[7] Xu T L, Lang X Z, Zhang X Y, et al. Study on the electric motor vibration signal de-noising using EMD correlation de-noising algorithm [J]. 2014, 18(5):599-603.

[8] Xu T L, Lang X Z, Zhang X Y, et al. Study on the electric motor vibration signal de-noising using EMD correlation de-noising algorithm [J]. 2014, 18(5):599-603.

[9] Smetana, Roland. Electric motor with elastic vibration damping rotor to shaft coupling [J]. Journal of the Acoustical Society of America, 78(2):820.

[10] Smetana, Roland. Electric motor with elastic vibration damping rotor to shaft coupling [J]. Journal of the Acoustical Society of America, 78(2):820.

[11] Cameron, J.R, Thomson, W.T, Dow, A.B. Vibration and current monitoring for detecting airgap eccentricity in large

induction motors [J]. Electric Power Applications Iee Proceedings B, 133(3):155-163.

[12] H.A. Toliyat, M.S. Arefeen, A.G. Parlos. A method for dynamic simulation of air-gap eccentricity in induction machines [J]. IEEE Transactions on Industry Applications, 1996, 32(4):910-918.

[13] A.J.M. Cardoso, E.S. Saraiva. Computer-aided detection of air gap eccentricity in operating three-phase induction motors by Park's vector approach [J]. IEEE Transactions on Industry Applications, 1993, 29(5):897-901.

[14] Thomson W T, Rankin D, Dorrell D G. On-line current monitoring to diagnose airgap eccentricity-an industrial case history of a large high-voltage three-phase induction motor[C]// 2002.

[15] Toliyat H A, Alnuaim N A. Simulation and detection of dynamic air-gap eccentricity in salient-pole synchronous machines[C]// 1999.

[16] M. Drif, A. J. M. Cardoso. Air gap Eccentricity Fault Diagnosis, in Three-Phase Induction Motors, by the Instantaneous Power Signature Analysis[C]// Tird IET International Conference on Power Electronics, Machines and Drives. 2006.

[17] 李剑峰. 异步电动机的振动与减振 [J]. 电机技术(3):61.

[18] 付兴娥, 曹冬青. 2 极电动机振动分析及对策 [J]. 上海大中型电机, 2009(1).

[19] 郑沛熙. 关于传动机械引起电机振动的减振方法分析与对策 [J]. 大众科技, 000(5):97-98.

[20] 郑沛熙. 关于传动机械引起电机振动的减振方法分析与对策 [J]. 大众科技, 000(5):97-98.

[21] 曹平. 1780 产线 E2 立辊电机异常振动分析与对策 [J]. 梅山科技(4):5-7.

[22] 刘意军. 高速电机振动异常分析及对策 [J]. 中国化工贸易(7).

[23] 叶日东. 15MW 发电机振动原因分析与对策 [J]. 中国设备工程(7):67-69.

[24] 王松. Y 系列三相异步电动机振动分析与抑制[D]. 山东大学, 2007.

[25] 罗隆满. 直流电动机振动分析与减振措施 [J]. 设备管理与维修, 2003(9):18-18.

[26] 张洪奎. 电机振动的原因分析及处理对策 [J]. 石油和化工设备, 2005, 8(3):28-29.

[27] 胡勇, 徐颖, 哈福民. 同步电机异步启动引起的压缩机振动分析及对策 [J]. 风机技术, 2009(3):67-68.

[28] 李丽娜, 孙宏昌, 阿曼, et al. 基于预见控制功能的直线伺服电机冲击振动故障分析与对策研究 [J]. 机床与液压, 2011, 39(17):135-137.

[29] 袁晓玲. 开关磁阻电动机振动分析及控制研究[D]. 河海大学, 2004.

[30] 向春德. 发电机定子铁芯穿心螺杆振动分析及对策 [J]. 中国设备工程, 2017(13).